PIV ANALYSIS OF THE BOTTOM GAP EFFECT ON THE FLOW AROUND A FIR TREE

J.P. Lee [1], S.J. LEE[2, c]

[1]School of Environmental Science and Engineering, Pohang University of Science and Technology, Pohang, 790-784, Korea
[2]Department of Mechanical Engineering, Pohang University of Science and Technology, Pohang 790-784, Korea
[c]Corresponding author: Tel.: +82542792169; Fax: +82542793199; Email: sjlee@postech.ac.kr

KEYWORDS:
Main subjects: flow visualization around a fir tree, shelter effect
Fluid: air
Visualization method(s): PIV (particle image velocimetry)
Other keywords: Windbreak, white fir tree, wind tunnel, PIV

ABSTRACT: Windbreak forest has been used for centuries for various purposes including reduction of wind speed, control of heat and moisture transfer and pollutant diffusion, improvement of climate and environment, or increase of crop yields. These functional effects of windbreaks are directly related to reduction of oncoming wind speed. There are several factors influencing on the leeward flow behind windbreak such as porosity, height and shape of windbreak, and so on. In present study, flow around a small white fir tree was investigated with varying bottom gap (a gap between the bottom of the tree canopy and the ground surface). Velocity fields around the tree which is placed in a closed-type wind tunnel were quantitatively measured using a PIV technique. Three different flow regions are observed behind the tree and each flow region exhibits different flow structure as a function of bottom gap ratio. Depending on the gap ratio, the aerodynamic porosity of the tree is changed and different turbulence structure is induced. These changes in the flow and turbulence structures around a tree significantly affect the shelter effect of the tree.

1 Introduction

For centuries, windbreaks have been widely used as natural wind fences to protect crops, orchard trees, and livestock in windy areas. In previous studies on artificial wind fences, fence porosity has been considered as the most important parameter in determining the flow around the wind fences (Cleugh, 1998). Many studies have been focused on the reduction of mean velocity in the wake behind a wind fence with varying fence porosity.

Raine and Stevenson (1977) measured the mean velocities and turbulence intensities behind various porous fences using a hot-wire anemometer. They classified the wake flow into two regions, bleed-flow dominant and displacement-flow regions. Guan et al. (2003) performed a wind tunnel test for a natural windbreak model consisting of trees and shrubs. They estimated the aerodynamic porosity and drag coefficient of the windbreak by measuring the surrounding wind speed. Torita and Satou (2007) measured wind speeds at several points around eight natural shelterbelts to investigate the wide shelterbelts. However, the variations in the spatial distributions of mean velocities and turbulence intensities of the wake behind the windbreaks could not be handled.

Hagen et al. (1981) numerically investigated the effects of width, height, porosity, and other parameters of two-dimensional fences using the k–ε turbulence model. Bourdin and Wilson (2008) compared the results of numerical simulations for windbreaks and homogeneous shelterbelts with experimental data. Rosendfeld et al. (2010) simulated the flow across several arrangements of trees by employing the steady Reynolds-averaged Navier–Stokes approximation. However, these previous numerical simulations simply assumed the windbreaks as homogeneous porous fences.

When windbreaks are made with trees, a gap between the bottom of the tree canopy and the ground surface exists because of the presence of the bottom trunk. This kind of bottom gap is also required

in the construction of artificial wind barriers for the transport of vehicles and labor workers at several passages. Kim and Lee (2002) investigated the flow fields and shelter effects of porous fences with various bottom gaps using a hybrid particle tracking velocimetry (PTV) velocity field measurement technique. They reported that the region of mean velocity reduction and the shelter effect decrease as the gap ratio increases. However, the results cannot be applied directly to predict the flow behind a real tree because a tree has irregular morphological structures.
In the present study, the flow around a fir tree was investigated experimentally with varying the bottom gap. The velocity fields of the wake behind the tree placed in a wind tunnel test section were quantitatively measured using particle image velocimetry (PIV) technique. The variations of shelter effect were estimated and discussed by analyzing the obtained whole velocity field information.

2 Experimental Methods

2.1 Tree model

Evergreen trees have been used to make windbreak forests for a long time. The stiff needles or soft foliage of evergreens can withstand strong winds, and the year-round cover stays intact through the cold winter season. Fir trees are commonly used as windbreaks because of their ability to withstand strong winds in high-temperature regions and to provide thick shelter zones. In the present study, a five-year-old white fir tree (Abides concolor) was used as the model tree. Figure 1 shows the configuration and measurement plane for the tree sample. The height (H) and width (W) of the model tree are 16 cm and 11 cm, respectively. The bottom gap (G) between the bottom of the tree canopy and the ground surface was varied to provide the bottom gap ratios of G/H = 0.0, 0.1, and 0.2. The optical porosity (β) of the model tree was estimated to be 0.07. The measurement section is the center vertical plane passing the center at the tree sample (Fig. 1).

2.2 Experimental set-up

All experiments were performed in a closed-return type wind tunnel, which has a test section of 0.72 m (*W*) x 0.65 m (*H*) x 8 m (*L*). Figure 1 shows the experimental setup and the coordinate

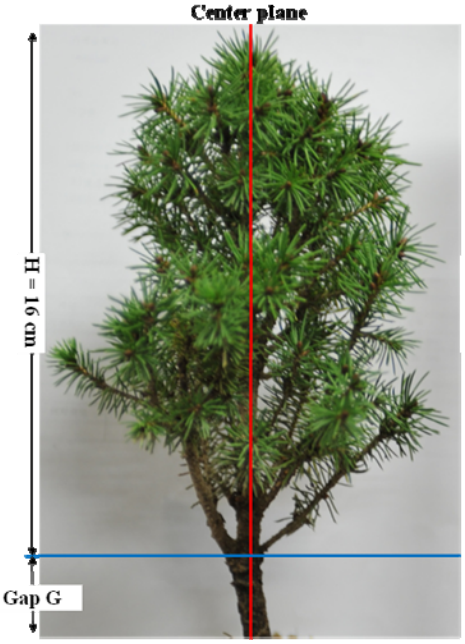

Fig. 1. A fir tree model with measurement plane.

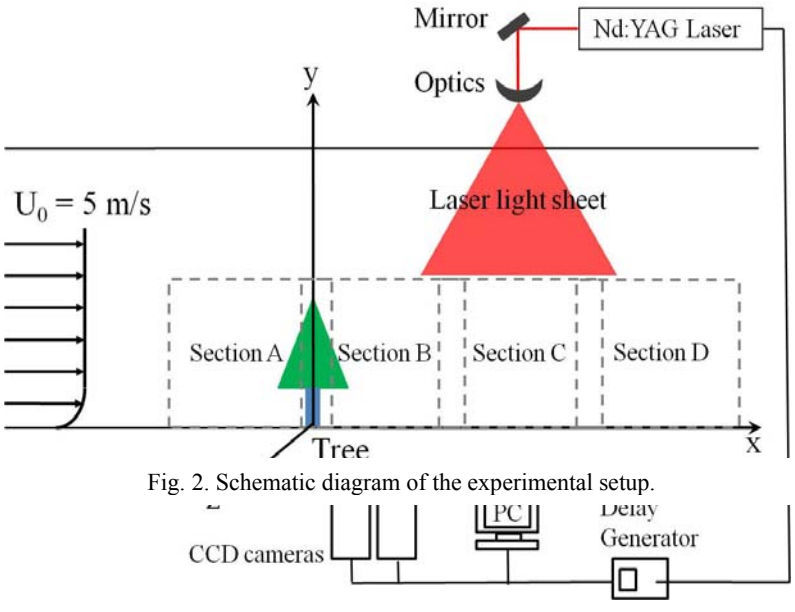

Fig. 2. Schematic diagram of the experimental setup.

system employed in the present study. The velocity fields of the flow around the tree sample placed in the wind tunnel test section were measured using a PIV technique. The PIV system consisted of a 200 mJ two-head Nd:YAG pulse laser, four CCD cameras with 2048×2048 pixels, a delay generator, mirrors and optical lenses, and a PC. A laser light sheet of 1 mm thickness was formed by passing the laser beam through cylindrical lenses and mirrors. Mirrors located at the roof of the wind tunnel illuminated the measurement sections, and olive oil droplets were used as tracer particles. Compressed air was supplied to the oil chamber to generate tracer particles using a Laskin nozzle. Oil droplets 1 to 3 μm in mean diameter were seeded into the wind tunnel test section.
In the PIV velocity field measurements, the velocity vector was extracted in each interrogation window of 32x32 pixels with a 50% overlap. Four hundred instantaneous velocity vector fields were obtained in each experimental condition. They were ensemble-averaged to obtain the spatial distributions of mean velocities and turbulence intensities.

The streamwise mean velocity and turbulence intensity profiles in the atmospheric boundary layer simulated inside the wind tunnel test section were measured with a hot-wire anemometer (TSI IFA-100) at the location of the tree sample, which is 4.5 m downstream from the leading edge of the test section. At each measurement point, 16,300 velocity data were acquired at a sampling rate of 2 kHz to 10 kHz after low-pass filtering at 800 Hz. The streamwise pressure gradient was nearly negligible due to the presence of corner fillets and small adjustable breathers located between the wind tunnel test section and the first diffuser.

Figure 3 shows the streamwise mean velocity and turbulence intensity profiles measured at the windbreak location. The mean streamwise velocity normalized by the reference velocity (U_{ref}) at the height of y_{ref} = 26 cm has a power-law profile (Eq. 1).

$$\frac{U(y)}{U_{ref}} = \left(\frac{y}{y_{ref}}\right)^{n} \quad \text{----------} \quad (1)$$

The velocity profile is well-fitted, with the power law exponent n = 0.16. The turbulence intensity near the ground surface is approximately 20%.

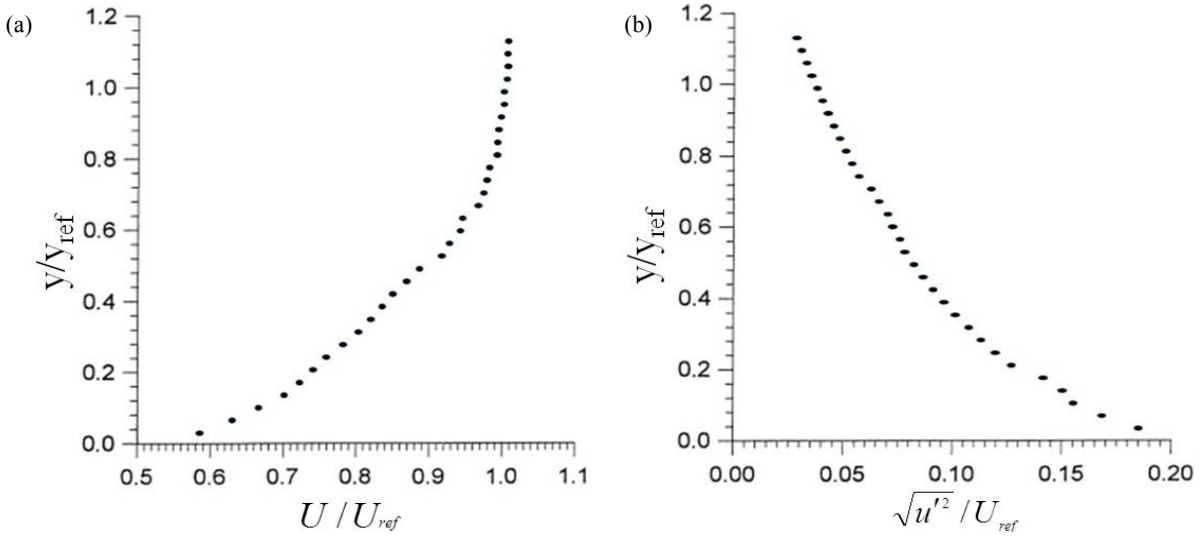

Fig. 3. Mean streamwise velocity and turbulence intensity profiles measured at the location of the model tree (a) mean velocity and (b) turbulence intensity

3 Results

3.1 Flow visualization

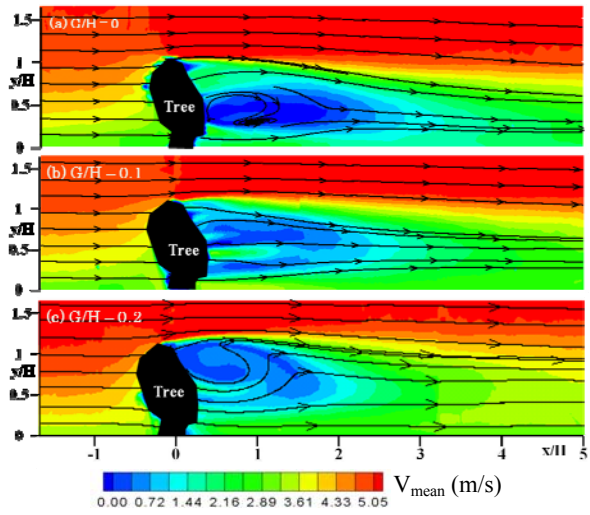

Fig. 4. Mean velocity contours and streamlines in the vertical center plane around a single tree.

(a) G/H = 0.0

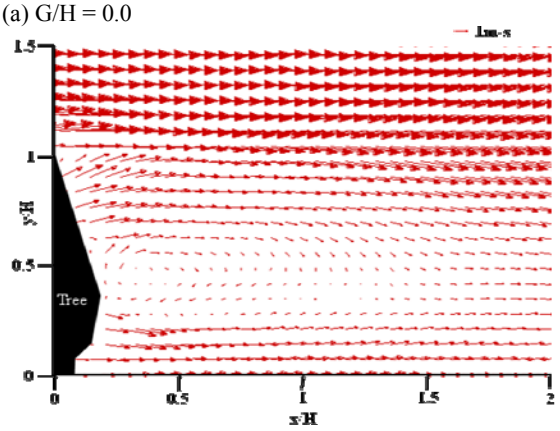

(b) G/H = 0.2

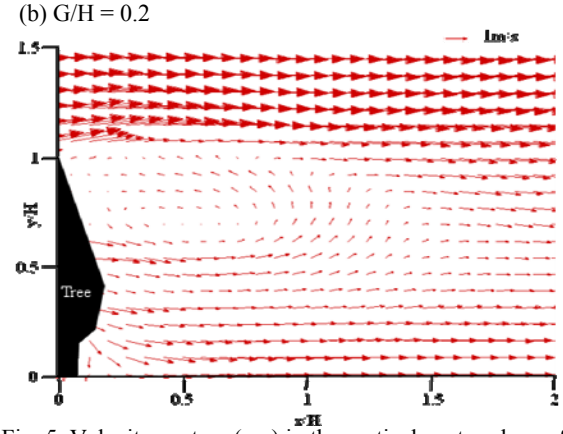

Fig. 5. Velocity vectors (u,v) in the vertical center plane of near wake behind the tree.

Figure 4 shows the contours of the mean velocity and streamlines of the flow around the tree model at three different bottom gap ratios. The axial velocity is largely reduced in the leeward of the tree canopy. However, the wind speed is increased in the near-ground region of the bottom gap in spite of ground proximity.

The flow pattern differs depending on the gap ratio. A recirculation flow is formed behind the canopy of the model tree in both cases of $G/H = 0$ and $G/H = 0.2$. At the bottom gap ratio of $G/H = 0.0$ (Fig. 4(a)), a clockwise large-scale recirculation zone is observed in the leeward side of the canopy in the vertical height ranging from $y/H = 0.3$ to 0.6 (Fig. 5(a)). Previous experimental and computational studies have reported the formation of a recirculation zone leeward of the dense shelterbelts with porosity of less than 0.3 (Gross, 1987; Heisler and Dewalle, 1988). The recirculation zone has a triangular shape bounded by a line connecting the crest of the shelterbelt and the reattachment point on the ground. However, the recirculation zone formed in the present study has an elliptical shape and the reattachment point does not exist on the ground surface. In the numerical simulations, the canopy of the tree models was assumed to be homogeneously porous. The solid internal structures of a real tree, such as boles, branches, leaves, and others were supposed to be negligible. Therefore, the recirculation zone of the present study was probably caused mainly by the internal structures of the real tree.

In the case of $G/H = 0.2$ (Fig. 4(c)), a counter-clockwise large-scale vortex is observed in the leeward side of the canopy in the vertical range of $y/H = 0.6$ to 1.0 (Fig. 5(b)). However, there is no large-scale recirculation flow in the case of $G/H = 0.1$ (Fig. 4(b)). This distinct flow structure will be discussed in the succeeding sections.

3.2 Flow structure

Figure 6 represents the mean streamwise and vertical velocity profiles taken from the velocity field data of Fig. 4 at the upstream location of $x/H = -0.5$. The presence of the tree slightly changed the mean streamwise velocity profiles, compared to that of the oncoming wind (Fig. 2(a)), which were measured without the tree model at the same location. In the upper region, above $y/H > 1$, the streamwise velocity is faster than that of the oncoming wind. However, in the lower region, below $y/H < 1$, the streamwise velocity is slower than that of the oncoming wind. When the gap ratio of

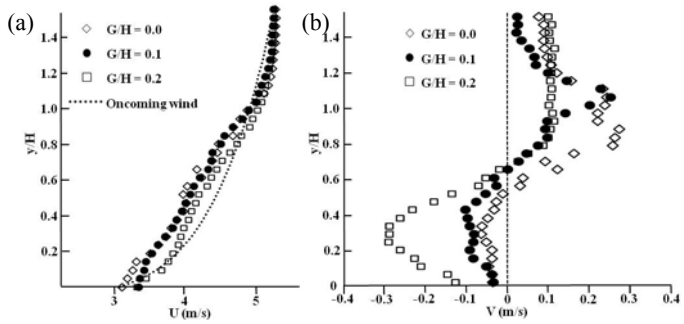

Fig. 6. Mean velocity profiles of (a) streamwise and (b) vertical velocity components measured at x/H = -0.5.

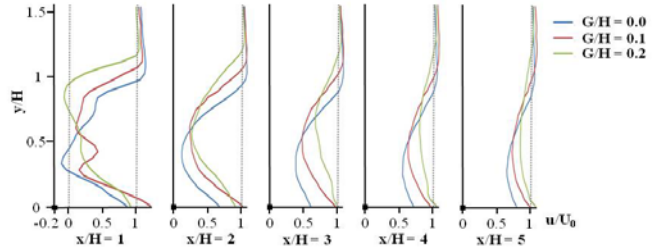

Fig. 7. Variations of mean streamwise velocity profiles along the x-direction

G/H = 0.2, the velocity reduction is smallest. However, the gap ratio of *G/H* = 0.0 exhibits the largest velocity reduction.

The vertical velocity component has negative values in the lower part of the tree,which is below the mid-height (0.5 < *y/H* < 0.7). This value indicates that the oncoming wind is divided into two opposite directions at this height of the tree. The separation point varies slightly depending on the length of the bottom gap. When the gap ratio increases, the negative vertical velocity increases, whereas the positive value decreases. In both cases of *G/H* = 0.0 and 0.1, the magnitudes of the negative vertical velocities are smaller than that of the positive values. The ground surface and bottom gap may have induced a sort of flow resistance and prevented the wind from heading to the ground.

When the gap ratio is *G/H* = 0.0, the vertical velocity has a maximum value in the top part of the canopy between *y/H* = 0.7 and 1.0. The oncoming wind mostly moves over or passes through the top part (Fig. 5(a)). This flow pattern may have caused the clockwise recirculation zone shown in Fig. 4(a). At the large gap ratio of *G/H* = 0.2, the vertical velocity has large negative values. In addition, the upward flow passing over the crest of the tree is smaller than the downward flow passing through the bottom gap. In this scenario, the bottom gap is wide enough for the flow to pass easily without significant flow resistance. The vertical velocity has maximum negative values in the region of *y/H* = 0.2 to 0.4. In the gap ratio of *G/H* = 0.2, most of the flow moves downward or passes through the lower part of the canopy (Fig. 5(b)). This kind of flow pattern seems to induce the counterclockwise recirculation flow shown in Fig. 4(c) and Fig. 5 (b).

Figure 7 shows the mean streamwise velocity profiles selected from the mean velocity field at five downstream locations. At *x/H* = 1, which is just behind the tree, the streamwise velocity has negative values for the cases of *G/H* = 0.0 and 0.1. This location belongs to the recirculation zone, as shown in Figs. 4 and 5. In addition, three different flow regions are observed behind the tree. These flow regions comprise two shear layers and one bleed flow region. The upper shear layer is developed from the top of the canopy, whereas the lower shear layer occupies the bottom gap in the near-wake region. The bleed flow passing though the canopy of the model tree makes up for the other region. In the upper shear layer (*y/H* > 0.7), the mean streamwise velocity increases as the gap ratio decreases. However, in the lower shear layer (*y/H* < 0.3), the streamwise mean velocity has the maximum value of *x/H* = 2, when the gap ratio is *G/H* =0.1. Beyond the downstream location of *x/H* = 2, the streamwise velocity increases as the gap ratio increases. Due to the expansion of the shear layers separated from the top and bottom edges of the tree canopy, the streamwise velocity profiles gradually approach the velocity profile (U_0) of the oncoming wind as the flow goes downstream, regardless of the gap ratio. Going downstream, the flow recovers its momentum deficit. This recovery rate increases as the gap ratio increases. Eventually, the flow might be restored to its original state at far downstream.

3.3 Shelter effect

Kim and Lee (2002) proposed a shelter parameter to quantify the shelter effect of a porous fence. This parameter not only reflects streamwise mean velocity but also includes vertical velocity. Although the vertical velocity component is relatively small compared with the streamwise velocity component, we need to consider the former to accurately evaluate the shelter effect. In this study, the following shelter parameter (Eq. 2) was employed to take into account the simulated atmospheric boundary layer at each position behind the bank of trees:

$$\psi_{(x,y)} = \frac{\left(\left|U_{(x,y)}\right| + \sqrt{u'^{2}_{(x,y)}} + \left|V_{(x,y)}\right| + \sqrt{v'^{2}_{(x,y)}}\right)}{\left(U_{ref\,(y)} + \sqrt{u'^{2}_{ref\,(y)}}\right)} \qquad (2)$$

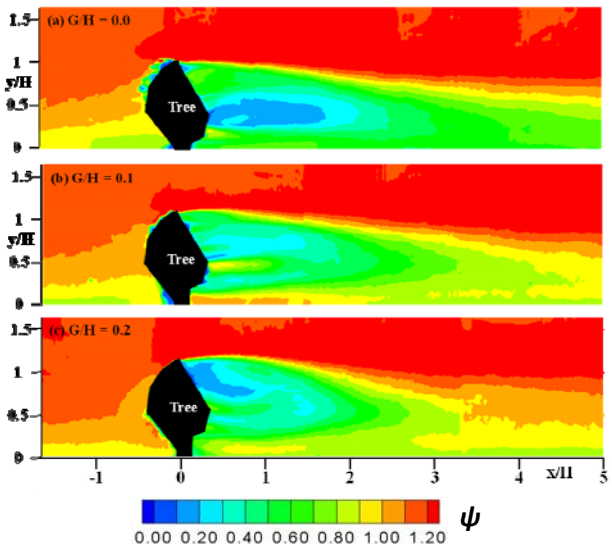

Fig. 8. Contour plots of the shelter parameter for three different gap ratios.

Figure 8 shows the contour plots of the shelter parameter according to the gap ratio. The contours of the shelter parameter in the upper shear layer look somewhat similar regardless of the gap ratio. The shelter parameter rapidly increases as the flow goes downstream. In the lower shear layer, the middle gap ratio of $G/H = 0.1$ has large values of shelter parameter because the gap flow passes the bottom gap at a high speed, as shown in Fig. 7. Considering the whole region, the gap ratio of $G/H = 0$ has the minimum value of shelter parameter. Moreover, the sheltered zone is widest among the three conditions tested in the present study.

4 Conclusions

The flow structure behind a fir tree was investigated with varying bottom gap ratios using a PIV velocity field measurement technique. Each flow region has different flow characteristics as a function of the gap ratio. The gap ratio of $G/H = 0$ is observed to have a clockwise large-scale recirculation flow in the near-wake region. However, the gap ratio of G/H = 0.2 makes a counterclockwise large-scale recirculation flow.

The shelter parameter representing the adverse shelter effect has a different spatial distribution according to the gap ratio. The gap ratio of $G/H = 0$ shows great shelter effect. However, the ratio of $G/H = 0.1$ has the worst shelter effect in the lower shear layer. The sheltering phenomenon is closely related to the modified flow characteristics, such as reduction of wind speed and turbulence intensity.

Acknowledgement

This work was supported by the Creative Research Initiatives (Diagnosis of Biofluid Flow Phenomena and Biomimic Research) of MOST/NRF of Korea.

References

1. Bourdin, P., Wilson, J.D., 2008. Windbreak aerodynamics: is computational fluid dynamics reliable?. Boundary-Layer Meteorol. 126,181–208

2. Gross, G., 1987. A numerical study of the air flow within and around a single tree. Boundary-Layer Meteorol . 40,311–327
3. Guan, D., Zhang, Y., Zhu, T., 2003. A wind-tunnel study of windbreak drag. Agric. For. Meteorol. 118,75–84
4. Hagen J.L., Skidmore E.L., Miller P.L., Kipp, J.E., 1981. Simulation of effect of wind barriers on airflow. Trans ASAE 24,1002–1008
5. Heisler, G.M., Dewalle D.R., 1988. Effects of windbreak structure on wind flow. Agric. Eco. Environ. 22, 41–69
6. Kim, H.B., Lee, S.J., 2002. The structure of turbulent shear flow around a two-dimensional porous fence having a bottom gap. J. Fluids Struct. 16, 317-329
7. Raine, J.K., Stevenson, D.C., 1977. Wind protection by model fences in a simulated atmospheric boundary layer. J. Wind. Eng. Ind. Aerodyn. 2, 17–39
8. Rosendfeld, M., Marom, G., Bitan, A., 2010. Numerical simulation of the airflow across trees in a windbreak. Boundary-Layer Meteorol. 135, 89–107
9. Torita, H., Satou, H., 2007. Relationship between shelterbelt structure and mean wind reduction. Agric For Meteorol. 145,186-194